

Theoretical Studies on the Interactions and Interferences of HIV-1 Glycoprotein gp120 and Its Coreceptor CCR5

Lin-tai Da[†] and Yun-Dong Wu^{*,†,‡,§}

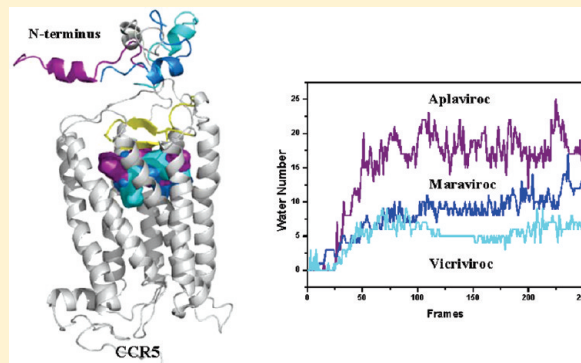
[†]School of Chemical Biology and Biotechnology, Laboratory of Chemical Genomics, Peking University Shenzhen Graduate School, Shenzhen, China

[‡]Department of Chemistry, The Hong Kong University of Science and Technology, Clear Water Bay, Kowloon, Hong Kong, China

[§]College of Chemistry, Peking University, Beijing, China

Supporting Information

ABSTRACT: The interaction between the HIV gp120 protein and coreceptor CCR5 or CXCR4 of the host cell is critical in mediating the HIV entry process. A model for the CCR5–gp120 complex has been developed. In the model, the N-terminus of CCR5 binds to three discontinuous domains of gp120, including the fourth conserved (C4) region, $\beta 19/\beta 20$ connecting loop, and V3 loop. The second extra-cellular loop (ECL2) of CCR5 also interacts with the crown part of the gp120 V3 loop. The bindings of the three CCR5 antagonists, maraviroc, aplaviroc, and vicriviroc, to the trans-membrane domain of CCR5 have been modeled. The bindings are found to affect the conformation of the ECL2 domain, which in turn drives the N-terminus of CCR5 to an altered state. Aplaviroc is more hydrophilic than maraviroc and vicriviroc, and its binding is more interfered by solvent, resulting in a quite different effect to the structure of CCR5 compared with those of the other two molecules. The above results are in accord with experimental observations and provide a structural basis for further design of CCR5 antagonists.



INTRODUCTION

The binding of CD4 induces conformational changes in HIV-1 gp120 to allow further involvement of a chemokine receptor CCR5 or CXCR4,^{1–9} resulting in the insertion of fusion peptide gp41 into the cell membrane and the fusion of virus and host cell membranes.^{10–16} Each single step described above is considered as a potential target for inhibiting viral entry.^{17–25}

NMR and mutagenesis studies reveal that several discontinuous domains of gp120 interact with the coreceptor CCR5,^{26–48} including the fourth conserved (C4) region, $\beta 19/\beta 20$ connecting loop, and V3 loop as shown in Figure 1. A binding model has been proposed. In this model the N-terminus of CCR5 (residues 2–15) interacts with two separated domains of gp120, the C4 domain and the base part of V3 loop, mainly through electrostatic interactions. The crown and stem domains of the V3 loop play critical roles in determining the coreceptor specificity of the virus. The N-terminus domain and the second extracellular loop (ECL2) of CCR5 are supposed to interact with the base and tip parts of the V3 loop of gp120, respectively.

As an important factor in mediating the HIV-1 entry process, the CCR5 antagonists have attracted a great deal of attention as novel anti-HIV-1 targets.⁴⁹ One CCR5 antagonist, maraviroc (Mar) (Selzentry; Pfizer, Scheme 1), has been approved by the United States Food and Drug Administration (USFDA) on

August 6, 2007 as a CCR5 antagonist.^{50,51} Clinical trials of aplaviroc (Apl) were stopped because of the potential toxic effects to the liver.^{52,53} Another small molecule, vicriviroc (Vic), exhibiting broad antiviral activity against diverse R5-tropic HIV-1 isolates in the nanomolar range, is currently in the clinical trials.^{54–58}

The mechanisms of the CCR5 antagonists in blocking HIV-1 entry have been extensively investigated.^{59–62} It has been established that the three small molecules (maraviroc, aplaviroc, and vicriviroc) sit in the pocket formed by the transmembrane (TM) domain of CCR5, surrounded by helices 1, 2, 3, 5, and 7.^{59–61} The gp120 binds to the extracellular domains of CCR5, suggesting that CCR5 antagonists inhibit viral entry mainly through allosteric effects.^{62,63}

Although the three CCR5 antagonists bind to the same hydrophobic pocket in CCR5, they occupy different subcavities,⁶⁴ which is reflected by their difference in regulating the signal transduction pathway of natural ligands.^{50,52–54} Apl exerts potent activity against a wide spectrum of laboratory and primary R5 HIV-1 isolates, including multidrug-resistant HIV-1 in vitro.⁵² Although it shows potent inhibition of the binding of the natural ligand MIP-1 α to CCR5, Apl only partially blocks the binding of MIP-1 β and

Received: September 2, 2010

Published: February 02, 2011

RANTES with a maximal inhibition of approximately 70%. Besides, the RANTES-induced chemotaxis during the CCR5 signal transductions was 70% retained at the IC₅₀ level of Apl (0.4nM).⁵² On the contrary, the other two inhibitors, Mar and Vic, prevent the binding of all three natural ligands equally well,^{50,54} indicating their distinct influences to the conformation of CCR5 compared with Apl.

Several theoretical efforts have been devoted to addressing the binding mode between gp120 and CCR5.^{65,66} Liu et al^{65,66} built a binding complex of gp120 and CCR5 in which the N-terminus of CCR5 makes direct contact with the bridging sheet domain of gp120. However, this does not agree with recent experimental results.²⁷ Docking and molecular dynamics studies^{67–70} have been applied to understand the binding modes between CCR5 and its antagonists or agonists, as well as the effects of these ligands on the structure of the trans-membrane domain of CCR5. However, to the best of our knowledge, an atomic-level understanding of the inhibition mechanism of CCR5 antagonists to the binding of gp120 is still lacking. More specifically, what is the origin of the different activities of the three antagonists in inhibiting natural ligands of CCR5? How does the binding of these antagonists induce conformational change of CCR5, especially the gp120-CCR5 binding interfaces?

Recently, we studied the conformational changes of gp120 induced by CD4 as well as anti-HIV inhibitors.⁷¹ Here, we extend

our studies to build a model for the interaction of gp120 with CCR5 and to report docking and molecular dynamics simulations to address the above questions.

METHODS AND MATERIALS

Homology Modeling of CCR5 Based on the Rhodopsin Structure. The CCR5 homology model was built by aligning the sequence of CCR5 against the sequence of bovine rhodopsin (PDB ID 1U19).⁷² The alignment was performed manually as indicated in Figure 2, ensuring the conserved GPCR residues matched with each other. The disulfide bond within the residues Cys20 and Cys269 was enforced to be formed by applying extra forces. Finally, the recently solved NMR structure of the N-terminus domain (residues 2–15, PDB ID 2RLL) of CCR5²⁷ was transplanted to the above model. The validation of the location of the N-terminus in the current CCR5 model can be obtained by comparing it with the recent crystal structure of CXCR4 (Figure S1 of the Supporting Information).⁷³ The disulfide bonds in the two structures are located in similar positions, although the ECL2 domains are in different orientations. The residues on the ECL2 of CXCR4 are much more hydrophilic than the counterparts of CCR5, resulting in more solvent exposure for the ECL2 domain in CXCR4. Figure 3 gives the final model of CCR5 in a liquid environment.

Setup of the CCR5 System in the Phospholipid Bilayer Environment. The CCR5 model was inserted into a membrane environment consisting of 228 palmitoyloleoylphosphatidylcholine (POPC) lipid molecules generated by an online module (http://charmm_gui.org). The embedded CCR5-POPC system was then solvated in the TIP3P water box⁷⁴ and neutralized by adding a proper number of ions. A molecule of cholesterol was added in order to stabilize the protein.⁷⁵ The final system contained 20171 solvent water molecules and 10 chloride ions (Figure 3).

The binding process of the three small molecules, Mar, Apl and, Vic, to the modeled CCR5 was studied by the AutoDock4 software package⁷⁶ with the aid of the AutoDockTools (ADT) interface. The flexibilities of several residues in the putative binding sites of the small molecules were also considered. Then the three obtained CCR5–antagonist complexes were inserted into the membrane environment in a similar way as above for CCR5 itself.

The parameters of the POPC lipid molecules and the three small inhibitors were obtained by using the Antechamber module in the AMBER10 program⁷⁷ (F1–F4 of the Supporting Information) and the GAFF force field.⁷⁸ The parameters of protein residues were assigned based on the AMBER ff03 force field.⁷⁹

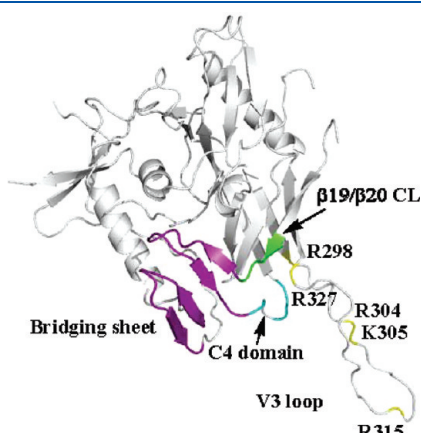
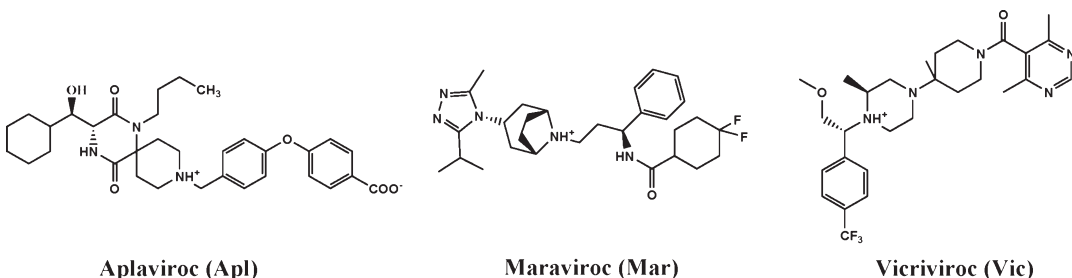


Figure 1. Several discontinuous domains of gp120 that are considered to affect the binding of CCR5. The R419, I420, K421, and Q422 of the β 19/ β 20 connecting loop (CL) are in green. The P437, P438, R440, G441, and Q442 located on the C4 domain are represented in cyan. Positively charged residues R298, R304, K305, R315, and R327 of the V3 loop are in yellow. The bridging sheet is in purple. Other parts of gp120 are in gray.

Scheme 1. Structures of Three CCR5 Antagonists



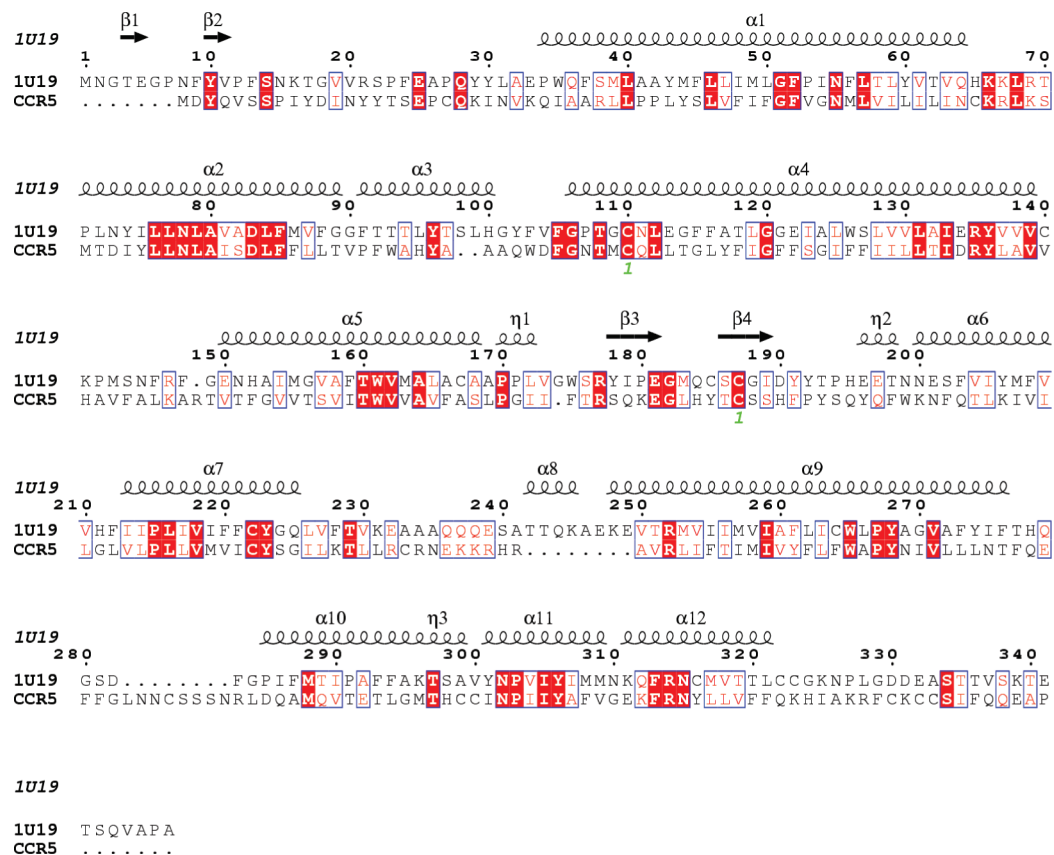


Figure 2. Sequence alignment of CCR5 (residues 1–339) against that of rhodopsin (PDB ID: 1U19). The conserved residues are highlighted in red, and the secondary structures are based on the template structure.

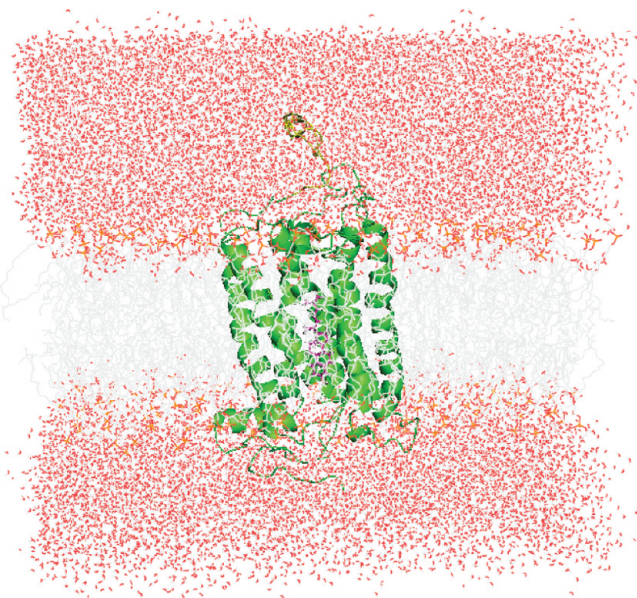


Figure 3. Embedded CCR5 within the palmitoyloleoylphosphatidylcholine (POPC) lipid layer (gray). The N-terminus domain of CCR5 is highlighted in yellow. The cholesterol is in purple.

Molecular Dynamics Setup. Standard molecular dynamics simulations were carried out for the four systems: CCR5, CCR5-Mar, CCR5-Apl, and CCR5-Vic. First, a two-stage energy minimization was applied to the four systems. In the first stage of

50000 steps, the receptor or receptor–antagonist system was restrained by a harmonic potential with a force constant of 32 kcal mol⁻¹ Å⁻², while the others (lipid and solvent) were relaxed. In the next 50000 steps, the whole system was relaxed. After the energy minimization, each system was subjected to a gradual heating process from 10 to 310 K in 200 ps. The receptor or receptor–antagonist system was constrained with a force constant of 32 kcal mol⁻¹ Å⁻². An anisotropic pressure scaling was applied, which is primarily intended for nonisotropic systems, such as membrane simulations. The final production run of 12 ns was performed at 310 K without any constraint. During the simulation, the bonds involving hydrogen atoms were constrained by applying the SHAKE algorithm.⁸⁰ The time step was 2 fs, and the particle mesh Ewald (PME) method^{81,82} was applied to calculate the long-range electrostatic interactions. All the simulations were performed with the AMBER10 program.⁷⁷

Flexible Docking of CCR5 with gp120. The docking of gp120 to CCR5 was performed using the Rosetta 3.0 software,⁸³ with the considerations of the flexibilities of both partners. The conformations of CCR5 were obtained from the CCR5 simulation at time intervals of 200 ps between 5 and 7 ns (10 snapshots), in which a conformational transition of the N-terminus domain of CCR5 occurred. As shown in Figure S2 of the Supporting Information, the N-terminus domain changed from perpendicular to the paper before 5 ns to parallel to the paper after 6 ns (Figure 4). On the other hand, the crystal structure of gp120 (PDB 2qad) was used as the starting structure for a 10 ns molecular dynamics study in order to relax the gp120 V3 loop domain. The conformations from the trajectory were assigned to

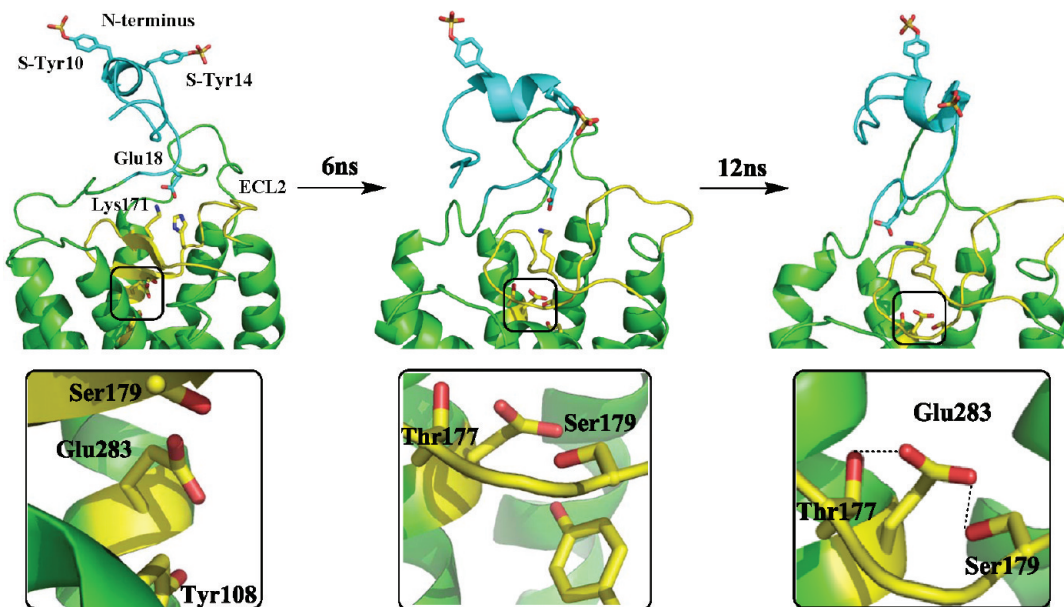


Figure 4. Structural change and critical interactions of CCR5 derived from molecular dynamics simulation. The N-terminus and the second extra-cellular loop of CCR5 are in cyan and yellow, respectively. The hydrogen bond network between the ECL2 and trans-membrane domains is shown below.

a total of 10 clusters, according to the rmsd changes. For each cluster, one random structure was selected for the subsequent protein–protein docking studies. Figure S3 of the Supporting Information shows the superimposed structures of the 10 conformations of gp120.

Protein–protein docking studies were conducted for every structure of CCR5 (10 in total) to each conformation of gp120 (10 in total), and for each gp120-CCR5 pair, 50 binding complexes were attempted. Finally, a total of 5000 docking complexes ($10 \times 10 \times 50$) were obtained. At the starting point of each docking process, the side chains of both partners were repacked first, followed by one cycle of rigid-body minimization and 50 cycles of Monte Carlo minimizations. The extra rotamers of the side chains from both proteins were included during the docking process.

Two criteria were applied to select the final gp120-CCR5 binding candidate. In criteria 1, the whole database, including the 5000 gp120-CCR5 binding complex, was ranked according to the value of the total score calculated by the Rosetta software. A total of 300 top conformations were filtered out for the next round. In criteria 2, in order to maximize the interaction interface between gp120 and CCR5, the 300 conformations obtained from the first round were further ranked according to the Lennard–Jones interaction items. Then, the second top pair of gp120 and CCR5, which is ranked at the top after the first round of selection, was used for the final analysis.

For comparison, docking studies were also conducted for the three CCR5–antagonist systems. The final structure of CCR5 in each simulation was used for docking under the same docking conditions as the Apo system.

Dynamic Cross-Correlation Map (DCCM). In order to evaluate the dynamic correlations between different domains, DCCM analyses were performed for the four CCR5 systems.^{84,85} The correlation coefficient, C_{ij} , between two atoms i and j , is defined as

$$C(i, j) = \frac{\langle \Delta R_i \times \Delta R_j \rangle}{[\langle \Delta R_i \times \Delta R_i \rangle \langle \Delta R_j \times \Delta R_j \rangle]^{1/2}}$$

where ΔR_i is the instantaneous fluctuation of the position of the i th atom with respect to its mean position. Positively correlated residues move in the same direction, namely $C(i, j) = 1$, whereas (negatively) anticorrelated residues move in the opposite direction, namely $C(i, j) = -1$. We use the coordinate derived at 5 ns as the reference state, and the subsequent coordinate sets are used for the DCCM analysis.

RESULTS AND DISCUSSION

The CCR5–gp120 Interaction Interface. The simulation of the CCR5 system shows that the N-terminus domain is restricted to a limited space (Figure 4), which is mainly due to two reasons. One is the constraint by the disulfide bond between Cys20 of N-terminus and Cys269 of the third extra-cellular loop (ECL3). The other is that the N-terminus domain can directly interact with the ECL2 and ECL3 domains through a Glu18-Lys171 salt-bridge and additional hydrophobic contacts. These factors stabilize the N-terminus domain of gp120 in an isolated state from the trans-membrane domain of CCR5, pointing the sulfated Tyr10 and Tyr14 to solvent. These two residues are supposed to directly bind to the positively charged residues from the V3 loop of gp120.²⁷

Figure 5 shows the CCR5–gp120 binding complex obtained by flexible docking. Compared with the crystal structure of gp120 (2qad), the docked state of gp120 exhibits an alternative conformation of V3 domain (See Figure S4 of the Supporting Information for details). In this complex, residues 7–15 of the N-terminus domain of CCR5 form an α helix, which binds to the root part of the V3 loop of gp120. A summary of the interactions between CCR5 and gp120 is listed in Table 1. As shown in panel A of Figure 5, the sulfated Tyr10 (S-Tyr10) binds to the site near Arg419 and Arg327, and Asp11 can form a salt bridge with Arg440 located on the C4 domain. The sulfated Tyr14 (S-Tyr14) is supposed to interact with Arg298 from the root part of the V3 loop. Some mutations on the C4 domain of gp120, such as Pro437, Arg440, Gly441, and Gln442, are found to affect the

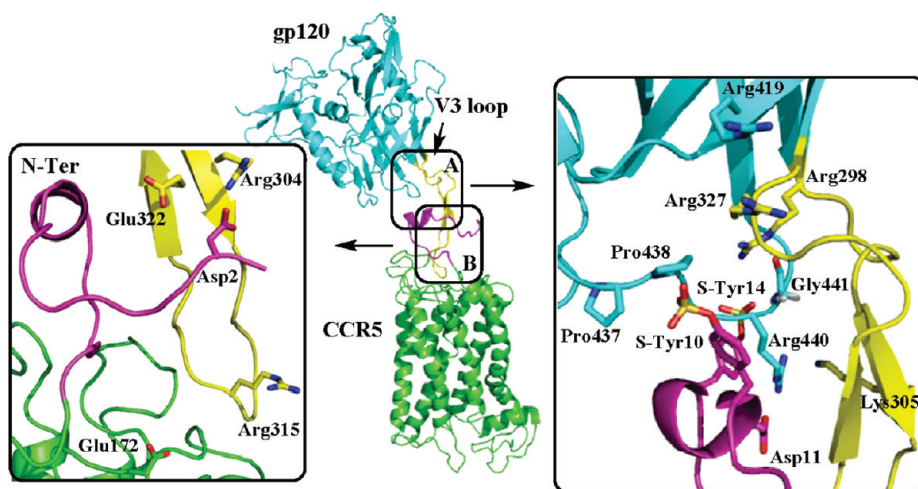


Figure 5. CCR5–gp120 complex derived from docking. The interfaces of CCR5–gp120 are highlighted in panels A and B. The V3 loop of gp120 and the N-terminus domain of CCR5 are in yellow and purple, respectively.

Table 1. Observed and Expected Interactions between gp120 and CCR5 in the Current Model

gp120	CCR5	location on gp120	location on CCR5	type
Observed Interactions				
Arg304	Asp2	V3 loop	N-terminus	salt bridge
Arg440	Asp11	C4 domain	N-terminus	salt bridge
Gly441	S-Tyr14	V3 loop; C4 domain	N-terminus	H-bond
Pro438	S-Tyr10	C4 domain	N-terminus	van der Waals
Expected Interactions				
Arg315	Glu172	V3 loop	ECL2	salt bridge
Arg327; Arg419	S-Tyr10	V3 loop; β 19/20	N-terminus	salt bridge
Arg298	S-Tyr14	V3 loop	N-terminus	salt bridge

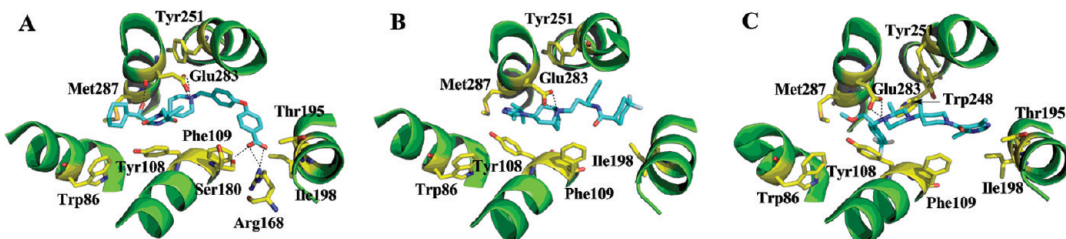


Figure 6. Docking mode between CCR5 and the three antagonists, Apl (A), Mar (B), and Vic (C).

CCRS binding,²⁸ which can be expected from our model. As shown in panel B of Figure 5, the tip part of the V3 loop can directly bind to the ECL2 domain of CCRS, which is consistent with the experimental observations.^{33–43} The Arg315 from V3 loop is expected to interact with Glu172 of CCRS. In addition, the current model suggests that residues 1–7 of CCRS also contribute to the binding affinity with gp120.

Binding Modes between CCR5 and the Three Antagonists. In the current study, the binding modes of CCR5 with the three antagonists were defined by combining the available site-directed mutagenesis analysis^{59–63} and the flexible docking studies with the AutoDock4 software. As shown in panel A of Figure 6, Apl sits in the largest hydrophobic cavity within the trans-membrane domain of CCR5. The CCR5–Apl complex is stabilized by intermolecular hydrogen bonds. A key interaction is a salt bridge formed between the tertiary nitrogen of Apl and the Glu283 located on the TM7 domain of CCR5. A network of

hydrogen bonds is formed among the residues Gly163 (not shown), Ser180, and Arg168. Apl also forms hydrogen bonds with the residues Glu283 and Asn252. Several hydrophobic residues and aromatic rings, such as Thr195 and Ile198 from TMS, Tyr108 and Phe109 from TM3, Trp86 from TM2, Met287 from TM7, and Tyr251 from TM6, have substantial hydrophobic contacts with the rest of the Apl molecule. It has been reported that mutations of the above residues reduce the inhibitory activity of the small molecule.^{43,59,61} Wang et al.⁶⁹ and Maeda et al.⁵⁹ provided an alternative interaction mode of Glu283, which formed hydrogen bonds with the hydroxy group of Apl, instead of the tertiary nitrogen atom. Li et al.⁷⁰ gave a quite different binding mode of Apl to the CCR5 pocket in which there is no obvious contact between Apl and TM2.

Similar to the CCR5–Apl complex, the antagonist Mar captures the same interaction between its tertiary nitrogen and Glu283 from TM7 of CCR5 as represented in panel B of Figure 6,

suggesting a general binding feature for this type of CCR5 antagonists. Compared with Apl, Mar has a smaller molecular size and interacts with fewer residues of CCR5. For example, the interferences of Met287 and Trp86 to the ligand binding are apparently reduced, supported by recent experimental observations.⁶¹ Other residues, including Tyr108 and Phe109 from TM3, Ile198 from TM5, and Tyr251 from TM6, are responsible for the tight binding of Mar to CCR5. Our subsequent molecular dynamics studies show that Tyr251 from TM6 can move into the Mar binding pocket, resulting in a hydrophobic contact with the phenol group of Mar. Kondru et al⁶¹ and Li et al⁷⁰ reported similar binding models for Mar.

As shown in panel C of Figure 6, the Glu283 also interacts with Vic through forming a salt bridge. Compared with the CCR5–Mar complex, Tyr251 binds more tightly with Vic due to the rotation of Tyr251 into the binding pocket; this explains the experimental observation that the Tyr251Ala mutation

Table 2. RMSD Values of the Trans-Membrane and Extra-Cellular Domains for Three Antagonist-Bound Systems^a

system	TM1	TM2	TM3	TM4	TM5	TM6	TM7	ECL2	Nter
Apl	3.07	2.12	1.83	1.83	2.00	2.70	2.21	6.16	16.5
Mar	2.32	2.08	2.20	1.72	1.69	2.78	2.02	3.76	11.60
Vic	2.85	1.83	1.83	1.97	2.51	2.30	2.23	3.16	16.2

^a The equilibrated structure of CCR5 (Figure 4) was used as the reference.

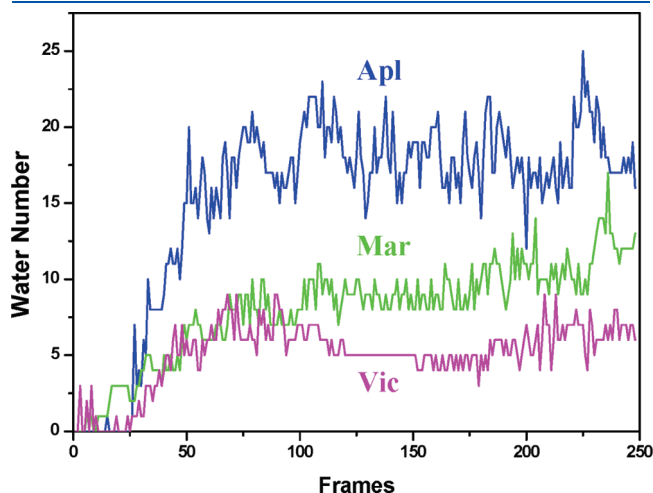


Figure 7. Number of water molecules around three CCR5 antagonists within 6 Å along the time frames: Apl (blue line), Mar (green line), and Vic (purple line).

results in the largest effect on the binding of natural ligands.⁶¹ Other hydrophobic residues, including Thr195, Ile198, Phe109, Tyr108, Met287, and Trp248, are also found to contact with Vic directly. The mutations of the above residues are found to dramatically reduce the inhibitory activities of the antagonist.⁶¹ A recent homology modeling study⁷⁰ based on the crystal structures of bovine rhodopsin and the human β 2-adrenergic receptor observed a similar binding mode between Vic and CCR5.

Conformational Changes of the N-terminus and ECL2 Domains of CCR5 Induced by the Binding of Antagonists. To investigate the effects of antagonist bindings to the trans-membrane domain of CCR5, a molecular dynamics simulation of 12 ns was performed for the three CCR5–antagonist systems. Table 2 summarizes the conformational changes of various parts of the domains of the CCR5 induced by the binding of the three antagonists using the equilibrated CCR5 structure as reference. While the trans-membrane helices TM1–7 all have some conformational changes, the largest conformational changes is to the N-terminus of the CCR5. Interestingly, contrary to Mar and Vic, Apl appears to cause a particularly large conformational change to the ECL2 domain of CCR5.

It has already been noted that Apl is larger and more hydrophilic than Mar and Vic. Thus, solvent effect can be significantly different for the three antagonists. Figure 7 shows the number of water molecules within 6 Å of the antagonists along the time frames. As the simulation progresses, the number of water molecules increases and then reaches a maximum of about 17, 8, and 5 for Apl, Mar, and Vic, respectively.

Figure 8 shows the CCR5 structures after a 12 ns simulation for the three systems. The conformational changes to the ECL2 and N-terminus are noticeable. It has been shown before that in the absence of an antagonist, the ECL2 of CCR5 is constrained in a closed form (Figure 4) due to a strong hydrogen bond network around residue Glu283, which includes Thr177, Ser179, Glu283, Tyr108, and several solvent molecules. However, the binding of Apl to CCR5 (Figure 8A) destroys the above hydrogen bond network by forming a salt bridge between the tertiary nitrogen atom of Apl and Glu283 of CCR5. The carboxyl group of Apl forms a stable hydrogen bond network with several residues of CCR5, including Arg168, Thr259, and Ser180 (bridged with a water molecule). In addition, the butane group of Apl further pushes the ECL2 away from its closed form. The above factors lead to dramatic conformational changes of the ECL2 domain (Figure 8A), which directly breaks the Glu18-Lys191 interaction between the N-terminus domain and the ECL2 domain. The loss of the interaction allows a flip of the N-terminus away from the

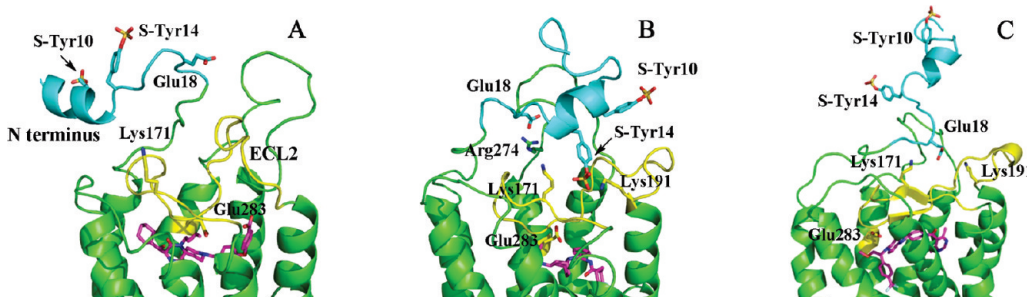


Figure 8. Effects of the binding of three antagonists, Apl (A), Mar (B), and Vic (C) to the structures of CCR5. The structures are derived at the simulation time of 12 ns for each system. The representations of CCR5 are similar to Figure 4.

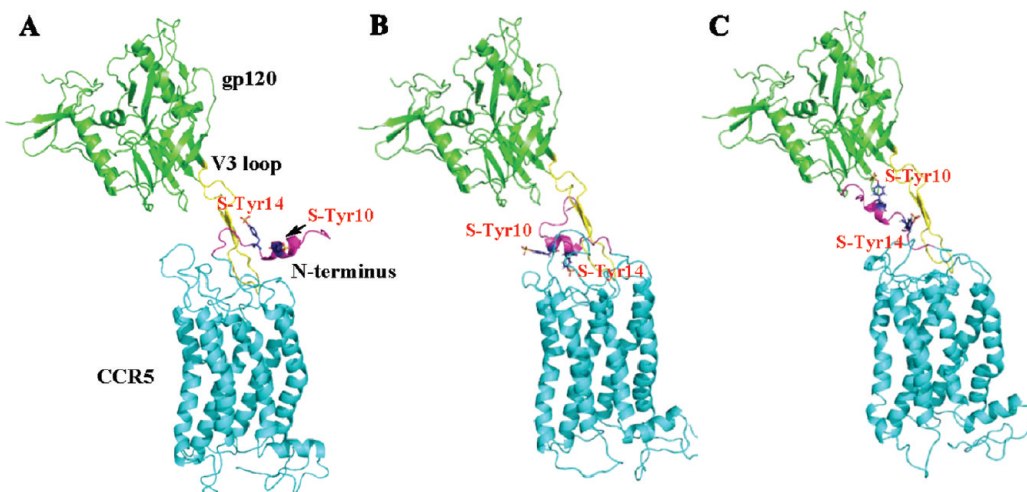


Figure 9. Docked CCR5–gp120 complexes under the binding of antagonists Apl (A), Mar (B), and Vic (C). The V3 loop of gp120 and the N-terminus domain of CCR5 are in yellow and purple, respectively. S-Tyr10 and S-Tyr14 of the N-terminus are shown in blue.

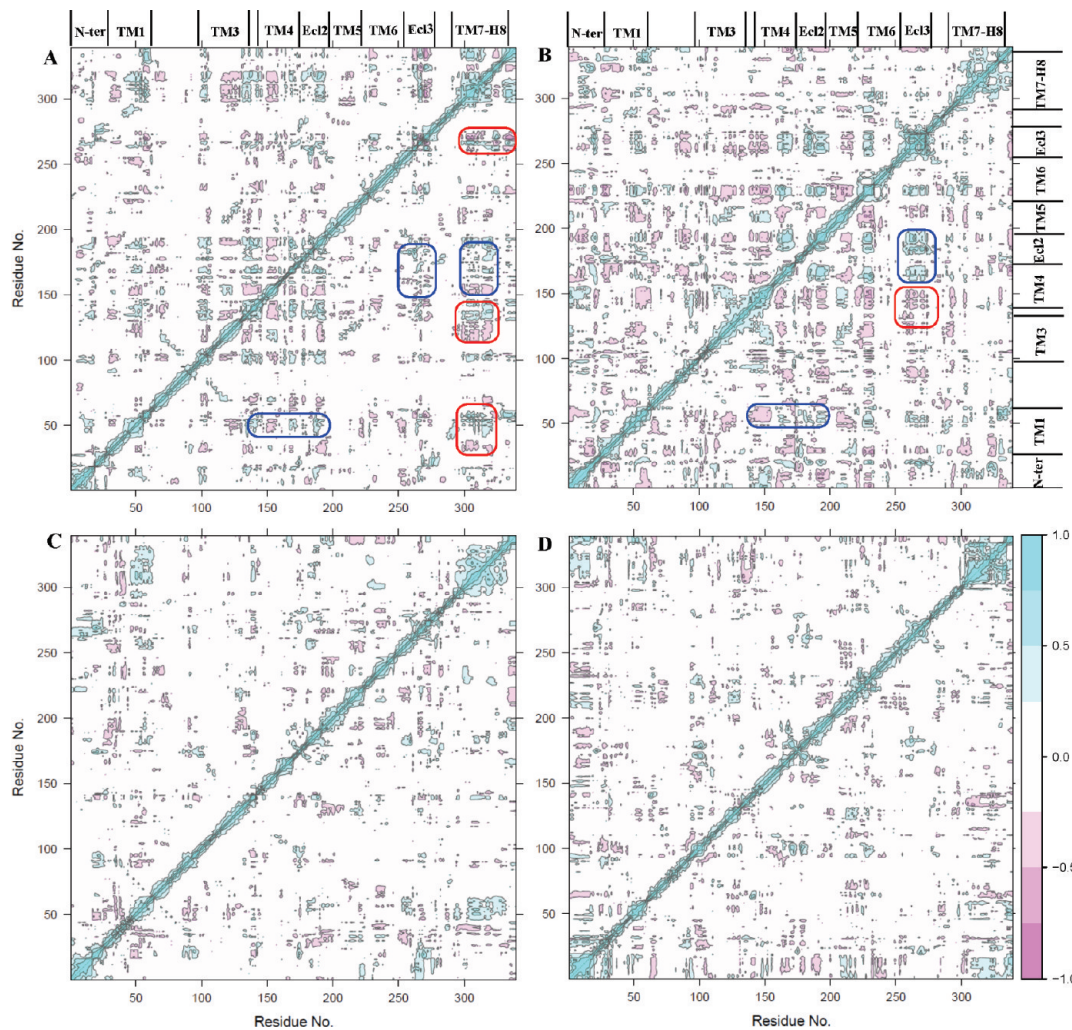


Figure 10. Dynamic cross-correlation map (DCCM) analyses for CCR5 (A), CCR5-Apl (B), CCR5-Mar (C), and CCR5-Vic (D).

ECL2 domain, resulting in an alternative state that is unlikely to accommodate gp120 (See next section).

Mar also forms a salt bridge with residue Glu283 using its tertiary nitrogen atom. However, this only partially destroys the

hydrogen bond networks associated with Glu283. The hydrogen bond between Glu283 and Ser179 remains. Several water molecules enter into the pocket to stabilize the salt bridge. The residues of E172–C178 of the ECL2 domain slightly rotate, which breaks the salt bridge between Lys171 and Glu18 but allows the formation of a new salt bridge between Glu18 and Arg274 (Figure 8B).

Interestingly, the phenyl group of Mar binds in a cavity adjacent to TM6. This significantly enlarges the distance between TM5 and TM6, so that the gap between the TM5 and TM6 can accommodate the C-terminal half of ECL2 domain, which in turn leaves room for the N-terminus to overlay with the ECL2 domain. As a result, a salt bridge between S-Tyr14 and Lys191 is formed (Figure 8B).

Although the binding of Vic to CCR5 breaks the hydrogen bond between Glu283 and Ser179, Glu283 forms a hydrogen bond with Thr177, using a water as a bridge. There are arrangements around the Lys171–Cys178 region. Lys171 forms a hydrogen bond with the backbone oxygen atom of residue Cys20. His181 forms a hydrogen bond with the backbone oxygen of residue Glu18. In addition, Glu18 also forms a salt bridge with Lys191 located on the C-terminal half of ECL2 (Figure 8C). Thus, considerable interactions between the ECL2 and N-terminus still remain.

Effects of Antagonist Bindings on the CCR5–gp120 Interaction. The conformational changes of the N-terminus and ECL2 domains of CCR5 induced by the binding of the three antagonists affect the recognition of gp120 by CCR5. Docking studies were carried out for the CCR5–gp120 interactions. As shown in Figure 9 for the docked structures of the CCR5–gp120 complexes, there are considerable losses of critical interactions between the N-terminus of CCR5 and the V3 loop of gp120, such as the electrostatic interactions between the sulfated Tyr10 and Tyr14 with the root part of V3 and C4 domain of gp120. In addition, the recognition between the tip part of V3 and the ECL2 domain of CCR5 is largely destroyed, reflected by the substantial reduced van der Waals interactions between the two proteins compared with the CCR5 (Table S1 of the Supporting Information). In the case of Apl (Figure 9A), the contact interface between the N-terminus of CCR5 and gp120 is completely impaired due to the rearrangement of the N-terminus domain. The docking studies qualitatively conclude that the CCR5–gp120 interaction is reduced by the binding of the antagonists to CCR5.

Effects of Antagonist Bindings to CCR5 on the Bindings of Natural Ligands (RANTES, MIP-1 α , and MIP-1 β). During the signal transduction process of the GPCR family, the couplings between the extra-cellular domains with the trans-membrane (TM) domains, such as TM6 and TM7, and intracellular Helix 8 (H8) are believed to be the major events.^{86,87} In order to study the effects of the small molecule antagonists on the signal transduction pathways mediated by CCR5, analysis of the dynamic cross-correlation map (DCCM) were performed. As shown in panel A of Figure 10 for the CCR5 system, there are obvious couplings between extra-cellular and trans-membrane domains. These include couplings of ECL2 with TM1 and TM7–H8, and ECL3 with TM4 and TM7–H8 domains. In addition, there are also couplings between TM7–H8 domains and TM1, TM3, and TM4 domains. However, these couplings are greatly decreased when Mar and Vic are bound to CCR5, as indicated in panels C and D of Figure 10, respectively. These suggest that the bindings of the two molecules rigidify the trans-membrane

domains of CCR5 and, therefore, inhibit the binding of the natural ligands.

In the case of Apl (Figure 10B), although the coupling between the ECL2 and the TM7–TM8 domains nearly disappears, the coupling between the ECL2 and TM1 domains remains. The coupling between the ECL3 and TM4 domains also exists. This may qualitatively explain why Apl allows RANTES-induced chemotaxis and CCRS internalization at its anti-HIV-1 activity-exerting concentration.⁵²

CONCLUSION

Molecular dynamics simulations and dockings indicate that several discontinuous domains of gp120, including the V3 loop, C4 domain, and β 19– β 20 connecting loop, interact with two separate domains of CCR5. The N-terminus of CCR5 can directly bind to the root parts of the gp120 V3 loop, C4 domain, and the β 19– β 20 connecting loop. The ECL2 domain of CCR5 binds to the crown domain of the gp120 V3 loop. The three CCR5 antagonists, Apl, Mar, and Vic, bind to the same largest pocket within the trans-membrane domain of CCR5. The binding can significantly affect the conformations of the ECL2 and N-terminus domains of CCR5, leading to reduced recognition of gp120 by CCR5. Molecular dynamics simulations indicate that there are considerable couplings between the extra-cellular (ECL2 and ECL3) and trans-membrane domains of CCR5. The bindings of Mar and Vic rigidify the trans-membrane domain of CCR5 so that the above couplings are inhibited and the bindings of natural ligands (RANTES, MIP-1 α , and MIP-1 β) to CCR5 are blocked. However, Apl only partially inhibits the above couplings, which qualitatively explains its different behavior from Mar and Vic in blocking the binding of the natural ligands.

ASSOCIATED CONTENT

S Supporting Information. Comparison of the CCRS model with the crystal structure of CXCR4 (Figure S1). The conformational transition of the N-terminus of CCR5 during simulation (Figure S2). The docking score calculated by Rossets 3.0 for the four systems (Table S1). The superimposed structures of the 10 conformations of gp120 used for docking (Figure S3). Rearrangement of the V3 loop induced by the binding of CCR5 (Figure S4). The AMBER parameters for small molecules (F1–F4). This material is available free of charge via the Internet at <http://pubs.acs.org>

AUTHOR INFORMATION

Corresponding Author

*E-mail: wuyd@pkusz.edu.cn.

ACKNOWLEDGMENT

We are grateful for the financial support of this research from the Research Grants Council of Hong Kong and National Science Foundation of China (N_HKUST623/04.663509).

REFERENCES

- (1) Lu, M.; Blacklow, S. C.; Kim, P. S. A trimeric structural domain of the HIV-1 transmembrane glycoprotein. *Nat. Struct. Biol.* **1995**, *2*, 1075–1082.
- (2) Choe, H.; Farzan, M.; Sun, Y.; Sullivan, N.; Rollins, B.; Ponath, P. D.; Wu, L.; Mackay, C. R.; LaRosa, G.; Newman, W.; Gerard, N.;

- Gerard, C.; Sodroski, J. The β -chemokine receptors CCR3 and CCR5 facilitate infection by primary HIV-1 isolates. *Cell* **1996**, *85*, 1135–1148.
- (3) Deng, H.; Liu, R.; Ellmeier, W.; Choe, S.; Unutmaz, D.; Burkhardt, M.; Di Marzio, P.; Marmon, S.; Sutton, R. E.; Hill, C. M.; Davis, C. B.; Peiper, S. C.; Schall, T. J.; Littman, D. R.; Landau, N. R. Identification of a major co-receptor for primary isolates of HIV-1. *Nature* **1996**, *381*, 661–666.
- (4) Doranz, B. J.; Rucker, J.; Yi, Y.; Smyth, R. J.; Samson, M.; Peiper, S. C.; Parmentier, M.; Collman, R. G.; Doms, R. W. A dual-tropic primary HIV-1 isolate that uses fusin and the β -chemokine receptors CCR-5, CCR-3, and CCR-2b as fusion cofactors. *Cell* **1996**, *85*, 1149–1158.
- (5) Feng, Y.; Broder, C. C.; Kennedy, P. E.; Berger, E. A. HIV-1 entry cofactor: Functional cDNA cloning of a seven-transmembrane, G protein-coupled receptor. *Science* **1996**, *272*, 872–877.
- (6) Wu, L.; Gerard, N. P.; Wyatt, R.; Choe, H.; Parolin, C.; Ruffing, N.; Borsetti, A.; Cardoso, A. A.; Desjardin, E.; Newman, W.; Gerard, C.; Sodroski, J. CD4-induced interaction of primary HIV-1 gp120 glycoproteins with the chemokine receptor CCR-5. *Nature* **1996**, *384*, 179–183.
- (7) Trkola, A.; Dragic, T.; Arthos, J.; Binley, J. M.; Olson, W. C.; Allaway, G. P.; Cheng-Mayer, C.; Robinson, J.; Madden, P. J.; Moore, J. P. CD4-dependent, antibody-sensitive interactions between HIV-1 and its co-receptor CCR-5. *Nature* **1996**, *384*, 184–187.
- (8) Wyatt, R.; Sodroski, J. The HIV-1 envelope glycoproteins: Fusogens, antigens, and immunogens. *Science* **1998**, *280*, 1884–1888.
- (9) Forsell, M. N. E.; Dey, B.; Mörner, A.; Svehla, K.; O'dell, S.; Högerkorp, C. M.; Voss, G.; Thorstensson, R.; Shaw, G. M.; Mascola, J. R.; Hedestam, G. B. K.; Wyatt, R. T. B cell recognition of the conserved HIV-1 co-receptor binding site is altered by endogenous primate CD4. *PLoS Pathog.* **2008**, *4*, e1000171.
- (10) Sattentau, Q. J.; Moore, J. P. Conformational changes induced in the human immunodeficiency virus envelope glycoprotein by soluble CD4 binding. *J. Exp. Med.* **1991**, *174*, 407–415.
- (11) Chan, D. C.; Fass, D.; Berger, J. M.; Kim, P. S. Core structure of gp41 from the HIV envelope glycoprotein. *Cell* **1997**, *89*, 263–273.
- (12) Tan, K.; Liu, J.; Wang, J.; Shen, S.; Lu, M. Atomic structure of a thermostable subdomain of HIV-1 gp41. *Proc. Natl. Acad. Sci. U. S. A.* **1997**, *94*, 12303–12308.
- (13) Weissenhorn, W.; Dessen, A.; Harrison, S. C.; Skehel, J. J.; Wiley, D. C. Atomic structure of the ectodomain from HIV-1 gp41. *Nature* **1997**, *387*, 426–430.
- (14) Furuta, R. A.; Wild, C. T.; Weng, Y.; Weiss, C. D. Capture of an early fusion-active conformation of HIV-1 gp41. *Nat. Struct. Biol.* **1998**, *5*, 276–279.
- (15) Zhu, P.; Liu, J.; J. B., Jr.; Chertova, E.; Lifson, J. D.; Grise, H.; Ofek, G. A.; Taylor, K. A.; Roux, K. H. Distribution and three-dimensional structure of AIDS virus envelope spikes. *Nature* **2006**, *441*, 847–852.
- (16) Liu, J.; Bartesaghi, Alberto.; Borgnia, M. J.; Sapiro, G.; Subramanian, S. Molecular architecture of native HIV-1 gp120 trimers. *Nature* **2008**, *455*, 109–113.
- (17) Chan, D. C.; Chutkowski, C. T.; Kim, P. S. Evidence that a prominent cavity in the coiled coil of HIV type 1 gp41 is an attractive drug target. *Proc. Natl. Acad. Sci. U. S. A.* **1998**, *95*, 15613–15617.
- (18) Chan, D. C.; Kim, P. S. HIV entry and its inhibition. *Cell* **1998**, *93*, 681–684.
- (19) Eckert, D. M.; Malashkevich, V. N.; Hong, L. H.; Carr, P. A.; Kim, P. S. Inhibiting HIV-1 entry: Discovery of D-peptide inhibitors that target the gp41 coiled-coil pocket. *Cell* **1999**, *99*, 103–115.
- (20) Eckert, D. M.; Kim, P. S. Design of potent inhibitors of HIV-1 entry from the gp41 N-peptide region. *Proc. Natl. Acad. Sci. U. S. A.* **2001**, *98*, 11187–11192.
- (21) Root, M. J.; Kay, M. S.; Kim, P. S. Protein design of an HIV-1 entry inhibitor. *Science* **2001**, *291*, 884–888.
- (22) Welch, B. D.; VanDemark, A. P.; Heroux, A.; Hill, C. P.; Kay, M. S. Potent D-peptide inhibitors of HIV-1 entry. *Proc. Natl. Acad. Sci. U. S. A.* **2007**, *104*, 16828–16833.
- (23) Esté, J.; Telenti, A. HIV entry inhibitors. *Lancet* **2007**, *370*, 81–88.
- (24) Kuritzkes, D. R. HIV-1 entry inhibitors: An overview. *Curr. Opin. HIV AIDS* **2009**, *4*, 82–87.
- (25) Tsibris, A. M.; Kuritzkes, D. R. Chemokine antagonists as therapeutics: Focus on HIV-1. *Annu. Rev. Med.* **2007**, *58*, 445–459.
- (26) Rizzuto, C. D.; Wyatt, R.; Hernandez-Ramos, N.; Sun, Y.; Kwong, P. D.; Hendrickson, W. A.; Sodroski, J. A conserved HIV gp120 Glycoprotein structure involved in chemokine receptor binding. *Science* **1998**, *280*, 1949–1953.
- (27) Huang, C.-C.; Lam, S. N.; Acharya, P.; Tang, M.; Xiang, S.-H.; Hussain, S. S.; Stanfield, R. L.; Robinson, J.; Sodroski, J.; Wilson, I. A.; Wyatt, R.; Bewley, C. A.; Kwong, P. D. Structures of the CCR5 N terminus and of a tyrosine-sulfated antibody with HIV-1 gp120 and CD4. *Science* **2007**, *317*, 1930–1934.
- (28) Rizzuto, C.; Sodroski, J. Fine definition of a conserved CCR5-binding region on the human immunodeficiency virus type 1 glycoprotein 120. *AIDS Res. Hum. Retro.* **2000**, *16*, 741–749.
- (29) Supaphiphat, P.; Thitithanyanont, A.; Paca-Uccaralertkun, S.; Essex, M.; Lee, T. H. Effect of amino acid substitution of the V3 and bridging sheet residues in human immunodeficiency virus type 1 subtype C gp120 on CCR5 utilization. *J. Virol.* **2003**, *77*, 3832–3837.
- (30) Comier, E. G.; Dragic, T. The crown and stem of the V3 loop play distinct roles in human immunodeficiency virus type 1 envelope glycoprotein interactions with the CCR5 coreceptor. *J. Virol.* **2002**, *76*, 8953–8957.
- (31) Hwang, S. S.; Boyle, T. J.; Lyerly, H. K.; Cullen, B. R. Identification of the envelope V3 loop as the primary determinant of cell tropism in HIV-1. *Science* **1991**, *253*, 71–74.
- (32) Hartley, O.; Klasse, P. J.; Sattentau, Q. J.; Moore, J. P. V3: HIV's switch-hitter. *AIDS Res. Hum. Retroviruses* **2005**, *21*, 171–189.
- (33) Atchison, R. E.; Gosling, J.; Montecarlo, F. S.; Franci, C.; Digilio, L.; Charo, I. F.; Goldsmith, M. A. Multiple extracellular elements of CCR5 and HIV-1 entry: Dissociation from response to chemokines. *Science* **1996**, *274*, 1924–1926.
- (34) Wu, L. J.; LaRosa, G.; Kassam, N.; Gordon, C. J.; Heath, H.; Ruffing, N.; Chen, H.; Humblia, J.; Samson, M.; Parmentier, M.; Moore, J. P.; Mackay, C. R. Interaction of chemokine receptor CCR5 with its ligands: Multiple domains for HIV-1 gp120 binding and a single domain for chemokine binding. *J. Exp. Med.* **1997**, *186*, 1373–1381.
- (35) Doranz, B. J.; Lu, Z. H.; Rucker, J.; Zhang, T. Y.; Sharron, M.; Cen, Y. H.; Wang, Z. X.; Guo, H. H.; Du, J. G.; Accavitti, M. A.; Doms, R. W.; Peiper, S. C. Two distinct CCR5 domains can mediate coreceptor usage by human immunodeficiency virus type 1. *J. Virol.* **1997**, *71*, 6305–6314.
- (36) Hill, C. M.; Kwon, D.; Jones, M.; Davis, C. B.; Marmon, S.; Daugherty, B. L.; DeMartino, J. A.; Springer, M. S.; Unutmaz, D.; Littman, D. R. The amino terminus of human CCR5 is required for its function as a receptor for diverse human and simian immunodeficiency virus envelope glycoproteins. *Virology* **1998**, *248*, 357–371.
- (37) Dragic, T.; Trkola, A.; Lin, S. W.; Nagashima, K. A.; Kajumo, F.; Zhao, L.; Olson, W. C.; Wu, L. J.; Mackay, C. R.; Allaway, G. P.; Sakmar, T. P.; Moore, J. P.; Madden, P. J. Amino-terminal substitutions in the CCR5 coreceptor impair gp120 binding and human immunodeficiency virus type 1 entry. *J. Virol.* **1998**, *72*, 279–785.
- (38) Rabut, G. E. E.; Konner, J. A.; Kajumo, F.; Moore, J. P.; Dragic, T. Alanine substitutions of polar and nonpolar residues in the amino-terminal domain of CCR5 differently impair entry of macrophage- and dualtropic isolates of human immunodeficiency virus type 1. *J. Virol.* **1998**, *72*, 3464–3468.
- (39) Genoud, S.; Kajumo, F.; Guo, Y.; Thompson, D.; Dragic, T. CCR5-mediated human immunodeficiency virus entry depends on an amino-terminal gp120-binding site and on the conformational integrity of all four extracellular domains. *J. Virol.* **1999**, *73*, 1645–1648.
- (40) Blanpain, C.; Doranz, B. J.; Vakili, J.; Rucker, J.; Govaerts, C.; Baik, S. S. W.; Lorthioir, O.; Migeotte, I.; Libert, F.; Baleux, F.; Vassart, G.; Doms, R. W.; Parmentier, M. Multiple charged and aromatic residues in CCR5 amino-terminal domain are involved in high affinity binding of

- both chemokines and HIV-1 Env protein. *J. Bio. Chem.* **1999**, *274*, 34719–34727.
- (41) Lee, B.; Sharron, M.; Blanpain, C.; Doranz, B. J.; Vakili, J.; Setoh, P.; Berg, E.; Liu, G.; Gug, H. R.; Durell, S. R.; Parmentier, M.; Chang, C. N.; Price, K.; Tsang, M.; Doms, R. W. Epitope mapping of CCR5 reveals multiple conformational states and distinct but overlapping structures involved in chemokine and coreceptor function. *J. Bio. Chem.* **1999**, *274*, 9617–9626.
- (42) Reeves, J. D.; Miamidian, J. L.; Biscone, M. J.; Lee, F. H.; Ahmad, N.; Pierson, T. C.; Doms, R. W. Impact of mutations in the coreceptor binding site on human immunodeficiency virus type 1 fusion, infection, and entry inhibitor sensitivity. *J. Virol.* **2004**, *78*, 5476–5485.
- (43) Maeda, K.; Das, D.; Yin, P.; Tsuchiya, K.; Ogata-Aoki, H.; Nakata, H.; Norman, R.; Hackney, L.; Takaoka, Y.; Mitsuya, H. Involvement of the second extracellular loop and transmembrane residues of CCR5 in inhibitor binding and HIV-1 fusion: Insights into the mechanism of allosteric inhibition. *J. Mol. Biol.* **2008**, *381*, 956–974.
- (44) Cormier, E. G.; Persuh, M.; Thompson, D. A. D.; Lin, S. W.; Sakmar, T. P.; Olson, W. C.; Dragic, T. Specific interaction of CCR5 amino-terminal domain peptides containing sulfotyrosines with HIV-1 envelope glycoprotein gp120. *Proc. Natl. Acad. Sci. U. S. A.* **2000**, *97*, 5762–5767.
- (45) Brower, E. T.; Schön, A.; Klein, J. C.; Freire, E. Binding thermodynamics of the N-terminal peptide of the CCR5 coreceptor to HIV-1 envelope glycoprotein gp120. *Biochemistry* **2009**, *48*, 779–785.
- (46) Cormier, E. G.; Tran, D. N. H.; Yukhayeva, L.; Olson, W. C.; Dragic, T. Mapping the determinants of the CCR5 amino-terminal sulfopeptide interaction with soluble human immunodeficiency virus type 1 gp120-CD4 complexes. *J. Virol.* **2001**, *75*, 5541–5549.
- (47) Farzan, M.; Choe, H.; Vaca, L.; Martin, K.; Sun, Y.; Desjardins, E.; Ruffing, N.; Wu, L. J.; Wyatt, R.; Gerard, N.; Gerard, C.; Sodroski, J. A tyrosine-rich region in the N terminus of CCR5 is important for human immunodeficiency virus type 1 entry and mediates an association between gp120 and CCR5. *J. Virol.* **1998**, *72*, 1160–1164.
- (48) Farzan, M.; Mirzabekov, T.; Kolchinsky, P.; Wyatt, R.; Cayabyab, M.; Gerard, N. P.; Gerard, C.; Sodroski, J.; Choe, H. Tyrosine sulfation of the amino terminus of CCR5 facilitates HIV-1 entry. *Cell* **1999**, *96*, 667–676.
- (49) Dhami, H.; Fritz, C. E.; Gankin, B.; Pak, S. H.; Yi, W.; Seya, M. J.; Raffa, R. B.; Nagar, S. The chemokine system and CCR5 antagonists: Potential in HIV treatment and other novel therapies. *J. Clin. Pharm. Ther.* **2009**, *34*, 147–160.
- (50) Dorr, P.; Westby, M.; Dobbs, S.; Griffin, P.; Irvine, B.; Macartney, M.; Mori, J.; Rickett, G.; Smith-Burchnell, C.; Napier, C.; Webster, R.; Armour, D.; Price, D.; Stammen, B.; Wood, A.; Perros, M. Maraviroc (UK-427,857), a potent, orally bioavailable, and selective small-molecule inhibitor of chemokine receptor CCR5 with broad-spectrum anti-human immunodeficiency virus type 1 activity. *Antimicrob. Agents Chemother.* **2005**, *49*, 4721–4732.
- (51) Carter, N. J.; Keating, G. M. Maraviroc. *Drugs* **2007**, *67*, 2277–2288.
- (52) Maeda, K.; Nakata, H.; Koh, Y.; Miyakawa, T.; Ogata-Aoki, H.; Takaoka, Y.; Shibayama, S.; Sagawa, K.; Fukushima, D.; Moravek, J.; Koyanagi, Y.; Mitsuya, H. Spirodiketopiperazine-based CCR5 inhibitor which preserves CC-chemokine/CCR5 interactions and exerts potent activity against r5 human immunodeficiency virus type 1 in vitro. *J. Virol.* **2004**, *78*, 8654–8662.
- (53) Watson, C.; Jenkinson, S.; Kazmierski, W.; Kenakin, T. The CCR5 receptor-based mechanism of action of 873140, a potent allosteric noncompetitive HIV entry inhibitor. *Mol. Pharmacol.* **2005**, *67*, 1268–1282.
- (54) Strizki, J. M.; Xu, S.; Wagner, N. E.; Wojcik, L.; Liu, J.; Hou, Y.; Endres, M.; Palani, A.; Shapiro, S.; Clader, J. W.; Greenlee, W. J.; Tagat, J. R.; McCombie, S.; Cox, K.; Fawzi, A. B.; Chou, C. C.; Pugliese-Sivo, C.; Davies, L.; Moreno, M. E.; Ho, D. D.; Trkola, A.; Stoddart, C. A.; Moore, J. P.; Reyes, G. R.; Baroudy, B. M. SCH-C (SCH 351125), an orally bioavailable, small molecule antagonist of the chemokine receptor CCR5, is a potent inhibitor of HIV-1 infection *in vitro* and *in vivo*. *Proc. Natl. Acad. Sci. U. S. A.* **2001**, *98*, 12718–12723.
- (55) Tsamis, F.; Gavrilov, S.; Kajumo, F.; Seibert, C.; Kuhmann, S.; Ketar, T.; Trkola, A.; Palani, A.; Clader, J.; Tagat, J.; McCombie, S.; Baroudy, Bahige.; Moore, J. P.; Sakmar, T.; Dragic, T. Analysis of the mechanism by which the small-molecule CCR5 antagonists SCH-351125 and SCH-350581 inhibit human immunodeficiency virus type 1 entry. *J. Virol.* **2003**, *77*, 5201–5208.
- (56) Tagat, J.; McCombie, S. W.; Nazareno, D.; Labroli, M. A.; Xiao, Y. S.; Steensma, R. W.; Strizki, J. M.; Baroudy, B. M.; Cox, K.; Lachowicz, J.; Varty, G.; Watkins, R. Piperazine-based CCR5 antagonists as HIV-1 inhibitors. IV. Discovery of 1-[(4,6-dimethyl-5-pyrimidinyl)-carbonyl]-4-[4-{2-methoxy-1(R)-4-(trifluoromethyl)phenyl}ethyl-3(S)-methyl-1-piperazinyl]-4-methylpiperidine (Sch-417690/Sch-D), a potent, highly selective, and orally bioavailable CCR5 antagonist. *J. Med. Chem.* **2004**, *47*, 2405–2408.
- (57) Strizki, J. M.; Tremblay, C.; Xu, S.; Wojcik, L.; Wagner, N.; Gonsiorek, W.; Hipkin, R. W.; Chou, C. C.; Pugliese-Sivo, C.; Xiao, Y. S.; Tagat, J. R.; Cox, K.; Priestley, T.; Sorota, S.; Huang, W.; Hirsch, M.; Reyes, G. R.; Baroudy, B. M. Discovery and characterization of vicriviroc (SCH 417690), a CCR5 antagonist with potent activity against human immunodeficiency virus type 1. *Anti. Age. Chemo.* **2005**, *49*, 4911–4919.
- (58) Ogert, R. A.; Ba, L.; Hou, Y.; Buontempo, C.; Qiu, P.; Duca, J.; Murgolo, N.; Buontempo, P.; Ralston, R.; Howe, J. A. Structure-Function analysis of human immunodeficiency virus type 1 gp120 amino acid mutations associated with resistance to the CCR5 coreceptor antagonist vicriviroc. *J. Virol.* **2009**, *83*, 12151–12163.
- (59) Maeda, K.; Das, D.; Ogata-Aoki, H.; Nakata, H.; Miyakawa, T.; Tojo, Y.; Norman, R.; Takaoka, Y.; Ding, J.; Arnold, G. F.; Arnold, E.; Mitsuya, H. Structural and molecular interactions of CCR5 inhibitors with CCR5. *J. Biol. Chem.* **2006**, *281*, 12688–12698.
- (60) Seibert, C.; Ying, W. W.; Gavrilov, S.; Tsamis, F.; Kuhmann, S. E.; Palani, A.; Tagat, J. R.; Clader, J. W.; McCombie, S. W.; Baroudy, B. M.; Smith, S. O.; Dragic, T.; Moore, J. P.; Sakmar, T. P. Interaction of small molecule inhibitors of HIV-1 entry with CCR5. *Virology* **2006**, *349*, 41–54.
- (61) Kondu, R.; Zhang, J.; Ji, C.; Mirzadegan, T.; Rotstein, D.; Sankuratri, S.; Dioszegi, M. Molecular interactions of CCR5 with major classes of small-molecule anti-HIV CCR5 antagonists. *Mol. Pharmacol.* **2008**, *73*, 789–800.
- (62) Baba, M.; Nishimura, O.; Kanzaki, N.; Okamoto, M.; Sawada, H.; Iizawa, Y.; Shiraishi, M.; Aramaki, Y.; Okonogi, K.; Ogawa, Y.; Meguro, K.; Fujino, M. A small-molecule, nonpeptide CCR5 antagonist with highly potent and selective anti-HIV-1 activity. *Proc. Natl. Acad. Sci. U. S. A.* **1999**, *96*, 5698–5703.
- (63) Dragic, T.; Trkola, A.; Thompson, D. A. D.; Cormier, E. G.; Kajumo, F. A.; Maxwell, E.; Lin, S. W.; Ying, W. W.; Smith, S. O.; Sakmar, T. P.; Moore, J. P. A binding pocket for a small molecule inhibitor of HIV-1 entry within the transmembrane helices of CCR5. *Proc. Natl. Acad. Sci. U. S. A.* **2000**, *97*, 5639–5644.
- (64) Stephenson, R. P. A modification of receptor theory. *Br. J. Pharmacol.* **1956**, *11*, 379–393.
- (65) Liu, S. Q.; Fan, S. X.; Sun, Z. R. Structural and functional characterization of the human CCR5 receptor in complex with HIV gp120 envelope glycoprotein and CD4 receptor by molecular modeling studies. *J. Mol. Model.* **2003**, *9*, 329–336.
- (66) Liu, S. Q.; Shi, X. F.; Liu, C. Q.; Sun, Z. R. Characterize dynamic conformational space of human CCR5 extracellular domain by molecular modeling and molecular dynamics simulation. *J. Mol. Struct.* **2004**, *673*, 133–143.
- (67) Xu, Y.; Liu, H.; Niu, C. Y.; Luo, C.; Luo, X. M.; Shen, J. H.; Chen, K. X.; Jiang, H. L. Molecular docking and 3D QSAR studies on 1-amino-2-phenyl-4-(piperidin-1-yl)-butanes based on the structural modeling of human CCR5 receptor. *Bioorg. Med. Chem.* **2004**, *12*, 6193–6208.
- (68) Fano, A.; Ritchie, W.; Carrieri, A. Modeling the structural basis of human CCR5 chemokine receptor function: From homology model building and molecular dynamics validation to agonist and antagonist docking. *J. Chem. Inf. Model.* **2006**, *46*, 1223–1235.
- (69) Wang, T.; Duan, Y. Binding modes of CCR5-targetting HIV entry inhibitors: Partial and full antagonists. *J. Mol. Graphics. Modell.* **2008**, *26*, 1287–1295.

- (70) Li, G.; Haney, K. M.; Kellogg, G. E.; Zhang, Y. Comparative docking study of anibamine as the first natural product CCR5 antagonist in CCR5 homology models. *J. Chem. Inf. Model.* **2009**, *49*, 120–132.
- (71) Da, L. T.; Quan, J. M.; Wu, Y. D. Understanding of the bridging sheet formation of HIV-1 glycoprotein gp120. *J. Phys. Chem. B* **2009**, *113*, 14536–14543.
- (72) Okada, T.; Sugihara, M.; Bondar, A. N.; Elstner, M.; Entel, P.; Buss, V. The retinal conformation and its environment in rhodopsin in light of a new 2.2 Å crystal structure. *J. Mol. Biol.* **2004**, *342*, 571–583.
- (73) Wu, B. L.; Chien, E. Y. T.; Mol, C. D.; Fenalti, G.; Liu, W.; Katritch, V.; Abagyan, R.; Brooun, A.; Wells, P.; Christopher Bi, F.; Hamel, D. J.; Kuhn, P.; Handel, T. M.; Cherezov, V.; Stevens, R. C. Structures of the CXCR4 chemokine GPCR with small-molecule and cyclic peptide antagonists. *Science* **2010**, *330*, 1066–1070.
- (74) Jorgensen, W. L.; Chandrasekhar, J.; Madura, J. D.; Impey, R. W.; Klein, M. L. Comparison of simple potential functions for simulating liquid water. *J. Chem. Phys.* **1983**, *79*, 926–935.
- (75) Hanson, M. A.; Cherezov, V.; Griffith, M. T.; Roth, C. B.; Jaakola, V.; Chien, E. Y. T.; Velasquez, J.; Kuhn, Peter.; Stevens, R. C. A specific cholesterol binding site is established by the 2.8 Å structure of the human β_2 -adrenergic receptor. *Structure* **2008**, *16*, 897–905.
- (76) Morris, G. M.; Huey, R.; Lindstrom, W.; Sanner, M. F.; Belew, R. K.; Goodsell, D. S.; Olson, A. J. AutoDock4 and AutoDockTools4: Automated docking with selective receptor flexibility. *J. Comput. Chem.* **2009**, *30*, 2785–2791.
- (77) Case, D. A.; et al. *AMBER10*; University of California: San Francisco, 2008.
- (78) Wang, J.; Wolf, R. M.; Caldwell, J. W.; Kollman, P. A.; Case, D. A. Development and testing of a general amber force field. *J. Comput. Chem.* **2004**, *25*, 1157–1174.
- (79) Duan, Y.; Wu, C.; Chowdhury, S.; Lee, M. C.; Xiong, G.; Zhang, W.; Yang, R.; Cieplak, P.; Luo, R.; Lee, T.; Caldwell, J.; Wang, J.; Kollman, P. A point-charge force field for molecular mechanics simulations of proteins based on condensed-phase quantum mechanical calculations. *J. Comput. Chem.* **2003**, *24*, 1999–2012.
- (80) Ryckaert, J. P.; Ciccotti, G.; Berendsen, H. J. C. Numerical integration of the cartesian equations of motion of a system with constraints: molecular dynamics of *n*-alkanes. *J. Comput. Phys.* **1977**, *23*, 327–341.
- (81) Darden, T.; York, D.; Pedersen, L. Particle mesh Ewald: An $N \cdot \log(N)$ method for Ewald sums in large systems. *J. Chem. Phys.* **1993**, *98*, 10089–10092.
- (82) Essmann, U.; Perera, L.; Berkowitz, M. L.; Darden, T.; Lee, H.; Pedersen, L. G. A smooth particle mesh Ewald method. *J. Chem. Phys.* **1995**, *103*, 8577–8593.
- (83) Gray, J. J.; Moughon, S.; Wang, C.; Schueler-Furman, O.; Kuhlman, B.; Rohl, C. A.; Baker, D. Protein–protein docking with simultaneous optimization of rigid-body displacement and side-chain conformations. *J. Mol. Biol.* **2003**, *331*, 281–299.
- (84) Ichiye, T.; Karplus, M. Collective motions in proteins: A covariance analysis of atomic fluctuations in molecular dynamics and normal mode simulations. *Proteins* **1991**, *11*, 205–217.
- (85) Swaminathan, S.; Harte, W. E.; Beveridge, D. L. Investigation of domain structure in proteins via molecular dynamics simulation: application to HIV-1 protease dimer. *J. Am. Chem. Soc.* **1991**, *113*, 2717–2721.
- (86) Ahuja, S.; Hornak, V.; Yan, E. C. Y.; Syrett, N.; Goncalves, J. A.; Hirshfeld, A.; Ziliox, M.; Sakmar, T. P.; Sheves, M.; Reeves, P. J.; Smith, S. O.; Eilers, M. Helix movement is coupled to displacement of the second extracellular loop in rhodopsin activation. *Nat. Struct. Mol. Biol.* **2009**, *16*, 168–175.
- (87) Bokoch, M. P.; Zou, Y. Z.; Rasmussen, S. G. F.; Liu, C. W.; Nygaard, R.; Rosenbaum, D. M.; Fung, J. J.; Choi, H. J.; Thian, F. S.; Kobilka, T. S.; Puglisi, J. D.; Weis, W.; Pardo, L.; Prosser, S.; Mueller, L.; Kobilka, B. K. Ligand-specific regulation of the extracellular surface of a G-protein-coupled receptor. *Nature* **2010**, *463*, 108–112.